PERFECT RECONSTRUCTION DFT MODULATED OVERSAMPLED FILTER BANK TRANSCEIVERS

Siavash Rahimi and Benoit Champagne

Department of Electrical and Computer Engineering, McGill University
Room 633, McConnell Engineering Building, 3480 University Street, Montreal, Quebec H3A 2A7
phone: + (1) 514-398-7110, email: siavash.rahimi@mail.mcgill.ca, benoit.champagne@mcgill.ca

ABSTRACT

This paper proposes a novel method for the design of perfect reconstruction (PR), discrete Fourier transform (DFT) modulated oversampled filter banks (FB) for application in multi-carrier transceiver systems. The PR property is guaranteed by enforcing a paraunitary constraint on the polyphase matrix of the transmit or receive sub-systems. The desired polyphase matrix is obtained via embedding of lower dimensional paraunitary building blocks, each expressed in terms of a limited set of design parameters through a factorization based on Givens rotations. These parameters are adjusted to minimize the stop-band energy of the subband filters and thus improve their spectral containment. The performance of the proposed FB is investigated in a multi-carrier transceiver application, where it is compared with OFDM and other recently proposed FB structures. Numerical results show that the proposed approach can lead to significant reduction in the bit error rate (BER), as compared to the benchmark approaches, when used in the presence of narrowband interference or frequency offset.

1. INTRODUCTION

Multicarrier modulation (MCM) is a method of transmitting a digital information sequence by splitting it into several components and sending each of these over separate carrier signals. In recent years, orthogonal frequency division multiplexing (OFDM), a form of MCM, has become the physical layer of choice for many wireless communication systems, e.g., IEEE 802.11, and IEEE 802.16. Despite its popularity, OFDM suffers from some important drawbacks including poor spectral containment due to low side-lobe attenuation, sensitivity to narrow-band noise [1], large peak-to-average power ratio (PAPR) [2], sensitivity to Doppler shift and frequency synchronization [3], and loss of efficiency caused by cyclic prefix.

As an alternative to OFDM, transceiver structures based on more general filter bank (FB) decompositions can benefit from improved spectral containment and thus provide an attractive approach for MCM applications. In this method, the data on the transmitter side is split into M parallel data channels, up-sampled by integer K and passed through a bank of transmit subband filters; the filter outputs are then summed and transmitted over the channel. At the receiver, the noisy data are passed through a bank of M receive subband filters, whose outputs are downsampled by K and equalized as needed to remove channel effects; finally, the original information sequence is reconstructed from the individually decoded data sub-streams.

In the context of MCM, the perfect reconstruction property refers to a situation where the output of the tandem combination of the transmit and receive FBs (i.e. ideal channel) is a delayed version of the input. Considering that in practice, non-ideal channels will introduce distortion and prevent the PR of the transmitted signal, some researchers have investigated the design property of nearly-perfect reconstruction (NPR) FBs for these applications

[4, 5]. However, the NPR design may require the use of more complex equalizers to combat intersymbol interference (ISI), which adds to the system's computational complexity [6]. In contrast, in the case of large number of subcarriers in PR FBs, the channel induced ISI can be easily removed by one-tap equalizer per subcarrier [7]. The main advantage for oversampled FBs (i.e. $K > M$) over critically sampled ones ($K = M$) is that in the former case, additional design freedom is available that can be used to obtain additional spectral containment and hence, better noise immunity within each subband. However, the use of oversampling leads to increased redundancy, and loss of spectral efficiency. Therefore, to remain competitive with existing OFDM systems, these redundancies in oversampled FBs should not exceed that introduced by the cyclic prefix in OFDM.

The main drawback of FB transceivers is their high complexity, both from the implementation and design perspectives. Indeed, to device an arbitrary M-channel FB transceiver, it is necessary to design and implement M transmit and M receive filters. To overcome this limitation, a class of FBs known as DFT modulated has been proposed [8, 9]. In this approach, the transmit and receive subband filters are all derived from a single prototype filter, that can be more efficiently designed due to the reduced number of free parameters. In addition, computationally efficient implementation of the resulting FB structure are possible with the help of time synchronized polyphase decompositions.

In this paper, we propose a design method for PR DFT modulated oversampled FB transceivers. It is shown that the PR property of the transceiver is equivalent to the paraunitary requirement on its polyphase matrix. This latter condition is enforced via embedding of paraunitary building blocks which are parameterized by a factorization in terms of Givens rotations. The FB design is formulated as a minimization problem over these parameters, where the objective function is the stop-band attenuation of the subband filters. The resulting prototype filter benefits from excellent spectral containment, that is high stop-band attenuation, and sharp transition band. In addition, unlike some other recently proposed methods, the oversampling factor K in our approach need not be a multiple of M, nor it is restricted to be even or odd; which provides additional design flexibility. The bit error rate (BER) performance of the proposed FBs in MCM transceiver applications is evaluated via extensive computer experiments. The result show increase immunity of the new system against narrowband interference (NBI) and colored noise, as compared to OFDM. Furthermore, because it employs sharp filters with much lower sidelobes, the proposed transceiver structure outperforms ODFM and other recently proposed methods when used in the presence of frequency offset.

The paper is organized as follows. Section 2 presents background information on PR DFT modulated oversampled FBs and the structure of their polyphase matrices. The parameterization of polyphase matrix and the proposed design method are developed in Section 3. Section 4 is devoted to the presentation of experimental results. Finally, Section 5 concludes the work. Regarding notations: Bold-faced letters indicate vectors and matrices. The paraconjugate operation on a matrix function $\mathbf{P}(z)$ is defined by $\tilde{\mathbf{P}}(z) = \mathbf{P}(z^{-1})^H$,
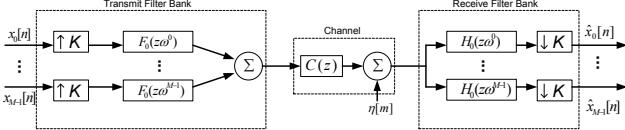
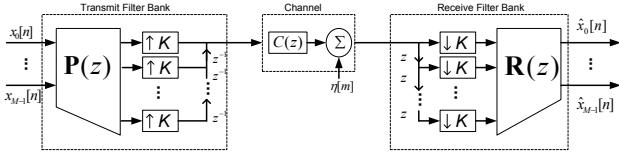Figure 1: DFT modulated oversampled filter bank transceiver

Figure 2: Oversampled filter bank polyphase representation

where the subscript H denotes the conjugate transpose. $\mathbf{I}_K$ denotes the $K \times K$ identity matrix. We say that a is congruent to b modulo m, or $a \equiv b \pmod{m}$, whenever $a - b$ is divisible by m.

2. DFT MODULATED FILTER BANKS

The proposed transceiver structure is depicted in Fig. 1, where $x_i[n]$ denote the transmitted data on the ith sub-channel. Parameters M and K represent number of subbands and upsampling/downsampling factor, respectively; as explained before, we consider oversampled FBs, where $K > M$. The transmission channel is modelled as an FIR filter with system function $C(z)$; the channel output is corrupted by additive noise $\eta[m]$. In DFT modulated FBs, the transmit and receive sub-band filters can be derived from common prototype filters of length D, with respective system functions[1] $F_0(z) = \sum_{n=0}^{D-1} f_0[n]z^{-n}$ and $H_0(z) = \sum_{n=0}^{D-1} h_0[n]z^n$ of length D. In this work, D is restricted to be a multiple of M and K, i.e. $D = d_M M = d_K K$, where d_M and d_K are positive integers. We also denote by P as the least common multiple of M and K, and therefore: $D = d_P P$ and $P = p_M M = p_K K$, with d_P, p_M and p_K integers. Defining $w = e^{-j2\pi/M}$, the transmit and receive filter for the ith subband ($i \in \{1, \ldots, M-1\}$) are respectively obtained as

$$F_i(z) = F_0(zw^i), \qquad H_i(z) = H_0(zw^i)$$

2.1 Polyphase Representation

Let us consider the polyphase representation of the ith transmit filter $F_i(z)$:

$$F_i(z) = \sum_{n=0}^{D-1} f_0[n] w^{-in} z^{-n} = \sum_{r=0}^{K-1} z^{-r} P_{i,r}(z^K),$$

$$P_{i,r}(z) = \sum_{q=0}^{d_K-1} f_0[Kq+r] w^{-i(Kq+r)} z^{-q}.$$

We define the $K \times M$ transmit polyphase matrix $\mathbf{P}(z)$, as $[\mathbf{P}(z)]_{r,i} = P_{i,r}(z)$. Similarly, the ith receive filter $H_i(z)$ admits the polyphase representation

$$H_i(z) = \sum_{n=0}^{D-1} h_0[n] w^{in} z^n = \sum_{r=0}^{K-1} z^r R_{i,r}(z^K),$$

$$R_{i,r}(z) = \sum_{q=0}^{d_K-1} h_0[Kq+r] w^{i(Kq+r)} z^q.$$

[1]For convenience in analysis, $H_0(z)$ is assumed non-causal; in practice, causality can be restored simply by adding a delay of $D-1$ samples in the receiver.

We also define the $M \times K$ receive polyphase matrix $\mathbf{R}(z)$, with entries $[\mathbf{R}(z)]_{i,r} = R_{i,r}(z)$. Using the above polyphase matrix representations in combination with Noble identities [10], the proposed transceiver in Fig. 1 can be represented as depicted in Fig. 2.

Next, we consider the factorization of the polyphase matrices $\mathbf{P}(z)$ and $\mathbf{R}(z)$ using an approach similar to that in [11, 8]. We begin by defining the $M \times M$ DFT matrix $\mathbf{W}$, with entries $[\mathbf{W}]_{i,j} = w^{ij}$, $i, j \in \{1, \ldots, M-1\}$. We also define the block matrices $\mathbf{L}_0$ and $\mathbf{L}_1(z)$, of respective size $D \times M$ and $K \times D$, as follows

$$\mathbf{L}_0 = [I_M, I_M, \ldots, I_M]^T,$$

$$\mathbf{L}_1(z) = [I_K, z^{-1}I_K, \ldots, z^{-(d_K-1)}I_K].$$

Considering first the transmit FB, we represent the D coefficients of the prototype filter $F_0(z)$ by means of diagonal matrix $\mathbf{\Gamma}_f = \mathrm{diag}(f_0[0], \ldots, f_0[D-1])$. Then, by using the fact $w^{M+c} = w^c$, we can write

$$\mathbf{P}(z) = \mathbf{L}_1(z)\mathbf{\Gamma}_f\mathbf{L}_0\mathbf{W} = \mathbf{U}(z)\mathbf{W} \tag{1}$$

where we define

$$\mathbf{U}(z) = \mathbf{L}_1(z)\mathbf{\Gamma}_f\mathbf{L}_0 \tag{2}$$

Proceeding as above, the following factorization can be developed for the receive FB: $\mathbf{R}(z) = \mathbf{W}^*\mathbf{L}_0^T\mathbf{\Gamma}_h\tilde{\mathbf{L}}_1(z)$, where $\mathbf{\Gamma}_h = \mathrm{diag}(h_0[0], \ldots, h_0[D-1])$.

In this paper, we assume that the transmit and receive prototype filters are paraconjugate of each other, $H_0(z) = \tilde{F}_0(z)$, which in turns implies that the polyphase matrices of the transmit and receive FB are also paraconjugate, i.e., $\mathbf{R}(z) = \tilde{\mathbf{P}}(z) = \mathbf{W}^*\tilde{\mathbf{U}}(z)$. Consequently, if $\mathbf{P}(z)$ can be made paraunitary, then the PR property of the transceiver system will be achieved since $\mathbf{P}(z)\mathbf{R}(z) = \mathbf{P}(z)\tilde{\mathbf{P}}(z) = \mathbf{I}_M$. In this case, and assuming an ideal channel with no receiver noise, i.e. $\mathbf{C}(z) = 1$ and $\eta[m] = 0$, the output of each subband on the receiver side will be an exact replica of the corresponding subband input on the transmitter with some integer delay d, or $\hat{x}_i[n] = x_i[n-d]$.

Finally, since $\mathbf{W}\mathbf{W}^* = \mathbf{I}_M$, we note from (1) that the paraunitariness of $\mathbf{P}(z)$ will follow automatically from that of $\mathbf{U}(z)$. This issue will be further addressed in Section 3, but first, we need to express the entries of matrix $\mathbf{U}(z)$ in terms of the coefficient of the prototype filter.

2.2 Structure of $\mathbf{U}(z)$

We begin by partitioning the $D \times M$ matrix $\mathbf{\Gamma}_f\mathbf{L}_0$ into the following format,

$$\mathbf{\Gamma}_f\mathbf{L}_0 = [\mathbf{F}_0^T | \mathbf{F}_1^T | \ldots | \mathbf{F}_{d_K-1}^T]^T,$$

where matrices $\mathbf{F}_q$, $q \in \{0, \ldots, d_K-1\}$, are of size $K \times M$ with entries

$$[\mathbf{F}_q]_{i,r} = \begin{cases} f_0[qK+i] & qK+i \equiv r \pmod{M} \\ 0 & \text{otherwise} \end{cases}, \tag{3}$$

Matrix $\mathbf{U}(z)$ (2) can then be expressed as

$$\mathbf{U}(z) = \mathbf{L}_1(z)[\mathbf{F}_0^T | \mathbf{F}_1^T | \ldots | \mathbf{F}_{d_K-1}^T]^T = \sum_{q=0}^{d_K-1} \mathbf{F}_q z^{-q}.$$

Introducing the change the variable $q = np_K + \alpha$, where $n \in \{0, \ldots, d_P-1\}$ and $\alpha \in \{0, \ldots, p_K-1\}$, we can rewrite $\mathbf{U}(z)$ as

$$\mathbf{U}(z) = \sum_{n=0}^{d_P-1}\sum_{\alpha=0}^{p_K-1} \mathbf{F}_{np_K+\alpha} z^{-np_K-\alpha}.$$

Noting that $p_K K = P$ and $P \equiv 0 \pmod{M}$, we obtain from (3) that

$$[\mathbf{F}_{np_K+\alpha}]_{i,r} = \begin{cases} f_0[nP+\alpha K+i] & \alpha K+i \equiv r \pmod{M} \\ 0 & \text{otherwise} \end{cases}. \tag{4}$$

We note that given a pair of indices (i, r), $[\mathbf{F}_{np_K+\alpha}]_{i,r}$ is identically zero except for possibly one specific value of $\alpha \in \{0, \ldots, p_K - 1\}$ which, if it exists, is denoted as $\alpha_{i,r}$ and satisfies

$$\alpha_{i,r}K + i \equiv r \pmod{M}, \qquad (5)$$

If this is the case, then it follows from (4) and (5) that

$$[\mathbf{U}(z)]_{i,r} = z^{-\alpha_{i,r}} \sum_{n=0}^{d_P-1} f_0[nP + \alpha_{i,r}K + i]z^{-np_K}; \qquad (6)$$

otherwise $[\mathbf{U}(z)]_{i,r} = 0$. Finally, by denoting

$$G_{i,r}(z) = \sum_{n=0}^{d_P-1} f_0[nP + \alpha_{i,r}K + i]z^{-n},$$

we can simplify equation (6) as

$$[\mathbf{U}(z)]_{i,r} = z^{-\alpha_{i,r}} G_{i,r}(z^{p_K}). \qquad (7)$$

3. PARAMETERIZATION OF PROTOTYPE FILTER

The design process starts with generating a parameterized matrix $\mathbf{U}(z; \theta)$ of the form (2), which is paraunitary. Then via (6), the prototype filter coefficients $f_0[n; \theta]$ can be obtained. Finally, the stop-band attenuation of this filter is minimized, based on the vector of parameters θ. Unfortunately, the elements of an arbitrarily generated paraunitary matrix $\mathbf{B}(z)$ will not match the $\mathbf{U}(z)$ in (2). $\mathbf{B}(z)$ must be restricted such that its components are compatible with $\mathbf{U}(z)$. The exact way of realising this depends on whether M and K are coprime.

3.1 M and K coprime

When M and K are coprime, $p_K = M$ and $p_M = K$ and a unique $\alpha_{i,r}$ in (5) exists for all the entries of $\mathbf{U}(z)$. We define two paraunitary matrices $\mathbf{D}_0(z) = \mathrm{diag}(z^{\alpha_{0,0}}, z^{\alpha_{1,0}}, \ldots, z^{\alpha_{p_M-1,0}})$ and $\mathbf{D}_1(z) = \mathrm{diag}(z^{\alpha_{0,0}}, z^{\alpha_{0,1}}, \ldots, z^{\alpha_{0,p_K-1}})$. Therefore, entries of the product $\mathbf{D}_0(z)\mathbf{U}(z)\mathbf{D}_1(z)$ can be written as

$$[\mathbf{D}_0(z)\mathbf{U}(z)\mathbf{D}_1(z)]_{i,r} = z^{\alpha_{i,0}} z^{\alpha_{0,r}} [\mathbf{U}(z)]_{i,r}. \qquad (8)$$

Using the pairs $(i, 0)$, $(0, r)$, and (i, r) in (5), we can show that

$$(\alpha_{i,0} + \alpha_{0,r} - \alpha_{i,r})K \equiv 0 \pmod{M}.$$

Therefore, introducing $\hat{\alpha}_{i,r} = \alpha_{i,0} + \alpha_{0,r} - \alpha_{i,r}$, we have $\hat{\alpha}_{i,r}K \equiv 0 \pmod{M}$. Thus, by using (7), we can rewrite equation (8) as

$$[\mathbf{D}_0(z)\mathbf{U}(z)\mathbf{D}_1(z)]_{i,r} = z^{\hat{\alpha}_{i,r}} G_{i,r}(z^{p_K}).$$

Since $0 \le \alpha_{i,r} < p_K$, $\hat{\alpha}_{i,r}$ can take only two values, i.e. 0 and p_K. Accordingly, the entries of $\mathbf{D}_0(z)\mathbf{U}(z)\mathbf{D}_1(z)$ are polynomials in z^{p_K}. It follows that when $\mathbf{B}(z)$ is an arbitrary matrix of order L with entries $[\mathbf{B}(z)]_{i,r} = \sum_{n=0}^{L-1} b_{i,r}[n]z^{-n}$,

$$\mathbf{D}_0(z)\mathbf{U}(z)\mathbf{D}_1(z) = \mathbf{B}(z^{p_K}) \text{ or } \mathbf{U}(z) = \tilde{\mathbf{D}}_0(z)\mathbf{B}(z^{p_K})\tilde{\mathbf{D}}_1(z).$$

Hence each entry of $\mathbf{U}(z)$ can be represented as

$$[\mathbf{U}(z)]_{i,r} = z^{-\alpha_{i,0}-\alpha_{0,r}}[\mathbf{B}(z^{p_K})]_{i,r}$$

By using (6), we can write

$$[\mathbf{B}(z^{p_K})]_{i,r} = \sum_{n=0}^{L-1} b_{i,r}[n]z^{-np_K} = z^{\hat{\alpha}_{i,r}} \sum_{n=0}^{d_P-1} f_0[nP + \alpha_{i,r}K + i]z^{-np_K} \qquad (9)$$

Depending on the value of $\hat{\alpha}_{i,r}$, the coefficients of the prototype filter for $i \in \{0, \ldots, K-1\}$, $r \in \{0, \ldots, M-1\}$, and $n \in \{1, \ldots, d_P - 1\}$, can be retrieved as

$$
\begin{cases}
\hat{\alpha}_{i,r} = 0 & \Rightarrow \begin{cases} f_0[nP + \alpha_{i,r}K + i] = b_{i,r}[n] \\ f_0[\alpha_{i,r}K + i] = b_{i,r}[0] \end{cases} \\[2em]
\hat{\alpha}_{i,r} = p_K & \Rightarrow \begin{cases} f_0[nP + \alpha_{i,r}K + i] = b_{i,r}[n-1] \\ f_0[\alpha_{i,r}K + i] = 0 \end{cases}
\end{cases} \qquad (10)
$$

Furthermore, the proper value of L can be determined to be $d_P - 2$.

3.2 M and K non-coprime

In this case, we can not find the proper $\alpha_{i,r}$ that satisfy (5) for some pair (i, r). Thus, the resulting $\mathbf{U}(z)$ consists of zero and non-zero entries. Let τ denote as the greatest common divisor or $\tau = KM/P$. According to [12], the paraunitariness of $\mathbf{U}_l(z)$, $l \in \{0, \ldots, \tau - 1\}$, which are defined as $p_M \times p_K$ submatrices of $\mathbf{U}(z)$, guarantees the paraunitariness of $\mathbf{U}(z)$. The structure of entries of each submatrix $\mathbf{U}_l(z)$ inside $\mathbf{U}(z)$ is as follows

$$[\mathbf{U}_l(z)]_{a,b} = [\mathbf{U}(z)]_{l+a\tau, l+b\tau},$$

where these entries are provided by (6). It is straightforward to show that for $i = l + a\tau$ and $r = l + b\tau$, the congruence relation (5) can be simplified to

$$\alpha_{l+a\tau, l+b\tau} p_M + a \equiv b \pmod{p_K}.$$

Because p_K and p_M are coprime, the $p_M \times p_K$ submatrices $\mathbf{U}_l(z)$ can be expressed in a similar fashion to (9). Therefore, to map each generated paraunitary matrix $\mathbf{B}_l(z)$ to the FB polyphase submatrix $\mathbf{U}_l(z)$, we can use the following equation

$$\mathbf{U}_l(z) = \tilde{\mathbf{D}}_0(z)\mathbf{B}_l(z^{p_K})\tilde{\mathbf{D}}_1(z).$$

Note that when M and K are non-coprime, τ different matrices $\mathbf{B}_l(z)$ should be generated.

3.3 Paraunitary Matrix Factorization

In order to maximize the spectral containment of the subband filters, generating a parameterized paraunitary matrix $\mathbf{B}(z)$ of size $p_M \times p_K$ is required. To this end, we first generate a square $p_M \times p_M$ paraunitary matrix $\boldsymbol{\Delta}(z)$, then apply the transformation $\mathbf{B}(z) = \boldsymbol{\Delta}(z)\mathbf{I}_{p_M \times p_K}$. With regards to generating $\boldsymbol{\Delta}(z)$, the decomposition for an $p_M \times p_M$ paraunitary matrix in terms of Givens rotation as in [13] is used. For a paraunitary matrix of order L, this decomposition can be written as

$$\boldsymbol{\Delta}(z) = \mathbf{R}_L \boldsymbol{\Lambda}(z) \mathbf{R}_{L-1} \boldsymbol{\Lambda}(z) \ldots \mathbf{R}_0.$$

Where $\boldsymbol{\Lambda}(z) = \mathrm{diag}(\mathbf{I}_{p_M-r_c}, z^{-1}\mathbf{I}_{r_c})$, with $r_c = \lfloor p_M/2 \rfloor$ and $\mathbf{R}_j$ is a unitary product of $p_M(p_M-1)/2$ Givens rotation matrices.

$$\mathbf{R}_j = \prod_{p=0}^{p_M} \prod_{q=p+1}^{p_M} \mathbf{G}_{p,q}$$

For each Givens rotation matrix $\mathbf{G}_{p,q}$, one parameter $\theta_{p,q}$ is required [14], Due to the fact that there are $p_M(p_M-1)/2$ different off-diagonal positions above the diagonal, the number of parameters required to construct a $p_M \times p_M$ paraunitary matrix is $(L+1)p_M(p_M-1)/2$. We note that one of the advantages of our method over [8] is the range of the parameters is limited to the interval $[0, 2\pi]$.

Method	J(dB)	First Sidelobe (dB)
Proposed	-35.42	-34
DFT-OSFB [8]	-35.29	-32
NPR-FB [4]	-30.51	-72
OFDM	-24.32	-13

Table 1: Spectral containment of different prototype filters

3.4 Optimization of Prototype Filter

The prototype filter coefficients $f_0[n;\theta]$ are optimized with respect to the vector of parameters θ. One of the benefits of PR FB transceiver is that in the process of filter design, the PR property relaxes any flatness condition on the passband region of the filter. Since the prototype filters are paraconjugate of each other, the pass band region of $|F_0(\omega;\theta)|^2$ is constant, where $F_0(\omega;\theta)$ is the discrete-time Fourier transform (DTFT) of $f_0[n;\theta]$ [10]. Therefore, good spectral containment can be achieved via minimization of the stop-band energy of the filter, denoted as the cost function,

$$J(\theta) = \frac{1}{2\pi} \int_{\omega_s}^{2\pi-\omega_s} |F_0(\omega;\theta)|^2 d\omega, \qquad (11)$$

where ω_s is the stop-band frequency. Since this optimization problem is a large-scale non-linear one, we used the Broyden-Fletcher-Goldfarb-Shanno (BFGS) algorithm[15], which is a quasi-Newton method, for minimizing the cost function.

4. SIMULATION

4.1 Prototype Filter Design

We design a prototype filter for the transceiver system with $M = 64$ subbands, oversampling factor $K = 72$, and filter length $D = 1728$. According to [8], for a given number of subbands M, better spectral features are obtained if the upsampling factor K and the length of the prototype filter D are increased. However, one must be careful as a higher K will reduce the bandwidth efficiency of the system. Likewise, a higher D will introduce more latency in the system and increase its computational complexity. These factors must be balanced carefully in order to maintain low latency, low computational complexity, and high bandwidth efficiency while benefiting from good spectral features.

Table 1 lists the stop-band attenuation $J(\theta)$ in (11) (when $\omega_s = \pi/M$) and first sidelobe attenuation of the proposed prototype filter, the OSFB prototype filter with $M = 64$, $K = 72$ and $D = 1728$ [8], the OFDM prototype filter with $M = 64$, and the NPR-FB with $M = 64$, $K = 64$ and $D = 1023$ [4]. Fig. 3 shows the frequency responses of these filters. Three key observations must be pointed out: from Table 1, the stop-band energy of the proposed scheme is the smallest among its counterparts; the transition from passband to stop-band, i.e. the rolloff, is much steeper for all of the FB approaches than for OFDM; the attenuations of the first two sidelobes of the proposed scheme are, respectively, about 34 and 48 dB, whereas the attenuations of the first two sidelobes of the OFDM system are 13 and 17 dB, respectively. These observations confirm that the proposed FB offer considerably better spectral containment than OFDM.

4.2 AWGN Channel

Fig. 4 shows the BER versus bit-energy-to-noise ratio (E_b/N_0) in the additive white Gaussian noise (AWGN) channel environment for the following transceivers: proposed scheme, the NPR cosine modulated FB [4], the OSFB transceiver in [8] and an OFDM system as described above . For all of the systems, QPSK modulation has been used for each of the subbands. To compare these mentioned schemes fairly, the redundancy caused by oversampling should be equal to the redundancy caused by cyclic prefix in OFDM
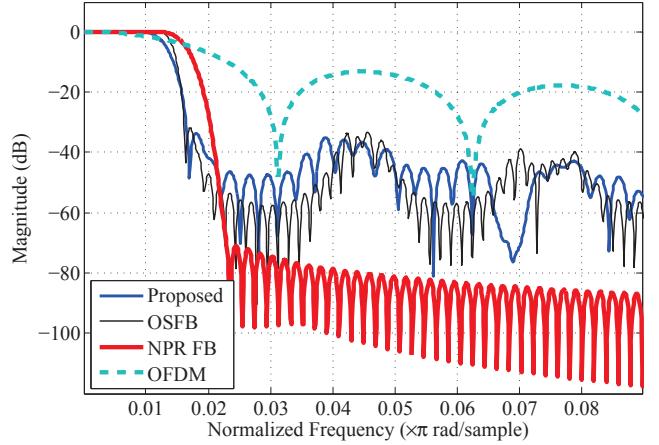

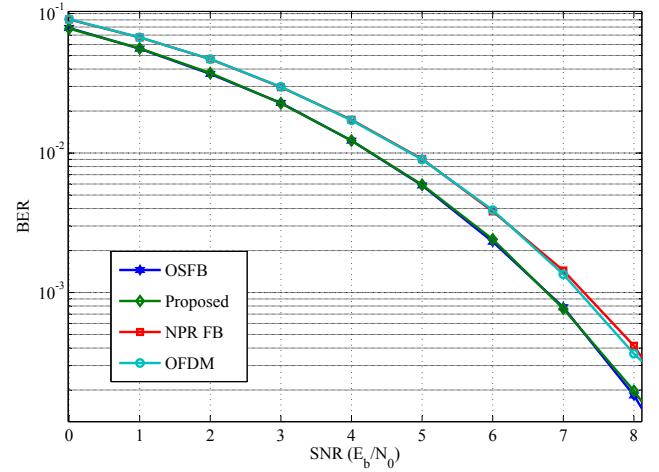Figure 3: Frequency response comparison

Figure 4: AWGN channel

(That is, with $M = 64$ and $K = 72$, the length of cyclic prefix is set to 8 in OFDM).

Therefore, the spectral efficiency is same over all of these schemes. In this regard, the spectral efficiency is $128/72$ *bpcu* (bit per channel use). Fig. 4 shows that both of the PR FB schemes exhibit a performance slightly better than NPR-FB and OFDM, when AWGN contaminates the communication channel. In this case, the simulated BER of the proposed scheme is indistinguishable to the theoretical BER for full-band QPSK modulation.

4.3 Narrowband Interference

To generate the NBI, we passed a white noise sequence through a narrow band-pass filter with a passband of width $2/M$.This simple interference model is realistic for narrowband FM (eg. cordless telephones), for low rate digital modulations, and for carrier feed through [1]. It is known that OFDM performance can be easily impaired by NBI. Due to the better spectral containment of the proposed FB transceiver as compared to the OFDM, we expect a better performance in the presence of NBI. In addition to NBI, white noise was added to channel output with a power level adjusted for BER= 10^{-3} as per results of Fig. 4. Fig. 5 shows the BER versus bit-energy-to-NBI ratio (E_b/I) of the same transceivers as explained in AWGN section. The results confirm that in this scenario, the proposed scheme outperforms OFDM, with a difference of about 3dB for BER=10^{-2}. However, at lower SIRs, the NPR-FB's performance is the best among different schemes, since NBI overshadows
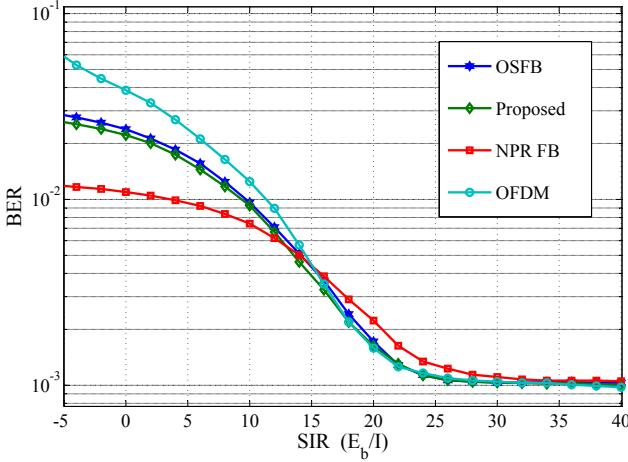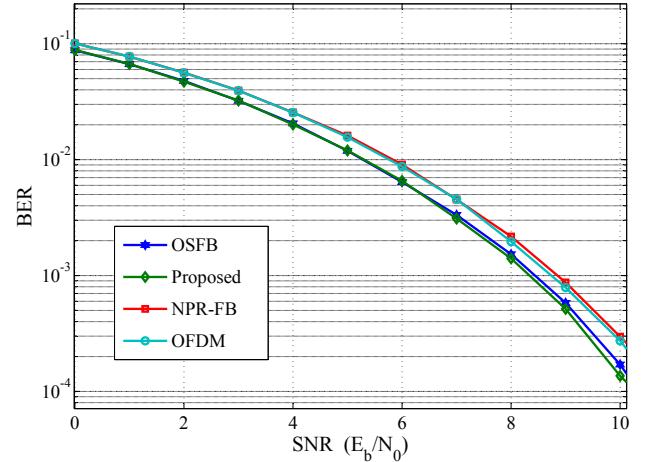
Figure 5: Narrowband interference

Figure 6: Frequency offset 5%

the distortion caused by NPR design and higher attenuation in side-lobes plays a main role in combating NBI. Note that at SIRs higher than 15dB, NPR distortion dominates and the NPR-FB has the highest BER.

4.4 Frequency Offset

It is known that sensitivity to frequency synchronization is one of the disadvantages of OFDM [3]. Small frequency offset in the OFDM receiver results in a reduction of useful signal amplitude, loss of orthogonality between subcarriers and consequently inter-carrier interference (ICI) from the neighbour subcarriers. Poor spectral characteristics of OFDM filters is the reason of high BER in the presence of frequency offset. Similarly, other MCM schemes are vulnerable against frequency offset, since the subbands are tightly spaced in the transmission bandwidth. To investigate this effect, we consider a scenario in which the receive FB is not exactly synchronized in frequency with the transmit FB. That is, we introduced a constant frequency offset on all the tone received. This offset, denoted as Δ_f, is measured as percent frequency deviation, relative to the width of a subband, i.e.intercarrier spacing. Fig. 6 shows the BERs of all previously compared schemes versus SNR in AWGN with $\Delta_f = 5\%$. As expected, the proposed transceiver outperforms OFDM and NPR-FB by more than 0.5 dB gain. The result of experiments for other values of Δ_f, e.g. 2% and 10%, follow the same trend.

5. CONCLUSION

In this paper, we proposed a design method for PR DFT modulated oversampled FBs transceivers. Paraunitary matrices were chosen as the polyphase matrices of the transmit and the receive FBs to ensure the PR property of the system. We were able to parameterize these matrices, based on factorization methods making use of Givens rotations. By applying BFGS algorithm, the stop-band energy attenuation of the prototype filters were minimized with respect to the rotation parameters to obtain a good spectral containment. The resulting filters benefit from steeper transition from pass-band to stop-band, lower stop-band energy, and lower in the side-lobe level, when compared with OFDM and some recently proposed FB transceivers. Numerical experiments show that the proposed FB also enjoys lower BER in the presence of NBI or frequency offset.

REFERENCES

[1] A. J. Coulson, "Bit error rate performance of OFDM in narrowband interference with excision filtering," *IEEE Trans. Wireless Commun.*, vol. 5, pp. 2484–2492, Sep. 2006.

[2] S. H. Han and J. H. Lee, "An overview of peak-to-average power ratio reduction techniques for multicarrier transmission," *IEEE Wireless Commun. Mag.*, vol. 12, pp. 56–65, Feb. 2005.

[3] T. Pollet, M. Van Bladel, and M. Moeneclaey, "BER sensitivity of OFDM systems to carrier frequency offset and wiener phase noise," *IEEE Trans. Commun.*, vol. 43, pp. 191–193, Feb. 1995.

[4] P. Martin-Martin, R. Bregovic, A. Martin-Marcos, F. Cruz-Roldan, and T. Saramaki, "A generalized window approach for designing transmultiplexers," *IEEE Trans. Circuits and Systems*, vol. 55, pp. 2696 –2706, Oct. 2008.

[5] L. Lin and B. Farhang-Boroujeny, "Cosine-modulated multi-tone for very-high-speed digital subscriber lines," *EURASIP J. Appl. Signal Process.*, vol. 2006, pp. 79–79, Jan. 2006.

[6] N. Benvenuto, S. Tomasin, and L. Tomba, "Equalization methods in ofdm and fmt systems for broadband wireless communications," *IEEE Trans. Commun.*, vol. 50, pp. 1413–1418, Sep. 2002.

[7] F. Beaulieu and B. Champagne, "One-tap equalizer for perfect reconstruction dft filter bank transceivers," in *Int. Sympo. on Signals, Systems and Electronics*, pp. 391–394, Aug. 2007.

[8] F. D. Beaulieu and B. Champagne, "Design of prototype filters for perfect reconstruction dft filter bank transceivers," *Signal Processing*, vol. 89, pp. 87–98, Jan. 2009.

[9] S.-M. Phoong, Y. Chang, and C.-Y. Chen, "DFT-modulated filterbank transceivers for multipath fading channels," *IEEE Trans. Signal Process.*, vol. 53, pp. 182 – 192, Jan. 2005.

[10] P. P. Vaidyanathan, *Multirate systems and filter banks*. Upper Saddle River, NJ, USA: Prentice-Hall, Inc., 1993.

[11] S. Weiss and R. W. Stewart, "Fast implementation of over-sampled modulated filter banks," *Electronics Letters*, vol. 36, pp. 1502–1503, Aug. 2000.

[12] Z. Cvetkovic and M. Vetterli, "Tight weyl-heisenberg frames in $l^2(z)$," *IEEE Trans. Signal Processing*, vol. 46, pp. 1256–1259, May 1998.

[13] X. Gao, T. Nguyen, and G. Strang, "On factorization of m-channel paraunitary filterbanks," *IEEE Trans. Signal Processing*, vol. 49, pp. 1433 –1446, Jul. 2001.

[14] G. Golub and C. Van Loan, *Matrix computations*. Johns Hopkins University Press, Baltimore, MD, 1996.

[15] J. Nocedal and S. J. Wright, *Numerical Optimization*. Springer, Berlin, August 2000.